

Cyclic liquefaction and pore pressure response of sand-silt mixtures

H.K. Dash*¹ and T.G. Sitharam²

¹*Department of Civil Engineering, College of Engineering and Technology (CET), Biju Patnaik University of Technology (BPUT), Bhubaneswar, India - 751003*

²*Department of Civil Engineering, Indian Institute of Science, Bangalore, India - 560 012*

(Received May 12, 2010, Accepted March 21, 2011)

Abstract. The effect of non-plastic fines (silt) on liquefaction and pore pressure generation characteristics of saturated sands was studied through undrained stress controlled cyclic triaxial tests using cylindrical specimens of size 50 mm diameter and height 100 mm at different cyclic stress ratios and at a frequency of 0.1 Hz. The tests were carried out in the laboratory adopting various measures of sample density through various approaches namely gross void ratio approach, relative density approach, sand skeleton void ratio approach, and interfine void ratio approach. The limiting silt content and the relative density of a specimen were found to influence the undrained cyclic response of sand-silt mixtures to a great extent. Undrained cyclic response was observed to be independent of silt content at very high relative densities. However, the presence of fines significantly influenced this response of loose to medium dense specimens. Combined analyses of cyclic resistance have been done using the entire data collected from all the approaches.

Keywords: stress controlled; gross void ratio; sand skeleton void ratio; interfine void ratio; limiting silt content; cyclic response.

1. Introduction

Recent findings by Lade and Yamamuro (1997), Thevanayagam (1998), Amini and Qi (2000), Polito and Martin (2001), Xenaki and Athanasopoulos (2003), Naeini and Baziar (2004), Ravishankar (2006), Sadek and Saleh (2007), Dash (2008) and Dash *et al.* (2010) reveal that sands with some amount of silt are much more liquefiable than clean sands and also that the pore pressure generation characteristics of silty sands are quite different from that of clean sands. Generation of excess pore water pressure in a soil mass reduces its strength and stiffness and as a result the stability of structures founded on the soil mass is significantly disturbed. This disturbance is acute during seismic loading. The effect of nonplastic fines on pore pressure generation and hence, the liquefaction characteristics of sandy soils have been studied extensively by many researchers in the recent past but the findings appear to be contradictory in nature. There is no agreement in the literature regarding the nature of variation of cyclic resistance of sandy soils with increase in fines

*Corresponding author, Reader, E-mail: hkbabool@gmail.com

content even at a particular measure of its density. This may be due to the fact that the sand structure is completely changed with the addition of fines. The present investigation involves the study of liquefaction and pore pressure generation characteristics of sand-silt mixtures through stress controlled cyclic triaxial tests conducted in the laboratory adopting various measures of their density through various approaches namely gross void ratio approach, relative density approach, sand skeleton void ratio approach, and interfine void ratio approach.

2. Materials used and their properties

2.1 Sand

Ahmedabad (India) sand was used in this study. The original sand contained around 9.8% of non-plastic fines (silt). It was wet sieved through a 75 micron IS sieve to obtain the clean sand. As per IS 1498 (1970) which is similar to ASTM standards, the clean sand is identified as poorly graded sand with symbol SP and it is quartzite in nature.

2.2 Silt

Quarry dust (< 75 microns) was used in this study as a substitute for silt. It is a byproduct of rubble crusher units in and around Bangalore. The grain size distribution as per IS 2720 (Part 4) of clean sand and the quarry dust (< 75 microns) are presented in Fig. 1. As per IS classification system the quarry dust is identified as inorganic silt with symbol ML. It is identified as derivatives of granite.

2.3 Sand-silt mixtures

Sand-silt mixtures were prepared by adding quarry dust (silt) in various percentages (by weight)

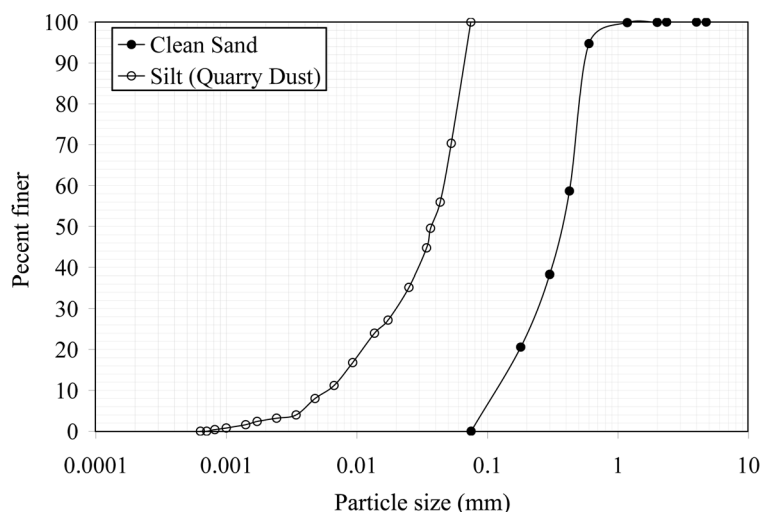


Fig. 1 Grain size distribution of clean sand and silt used in this study

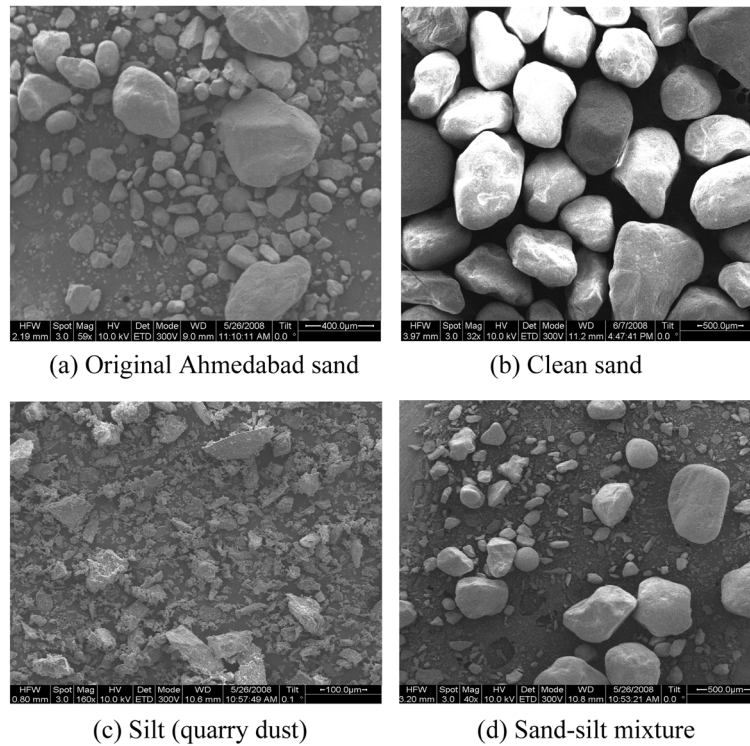


Fig. 2 Scanning electron microscopic view of the materials tested in the laboratory

to the clean sand. To avoid particle segregation, dry mixing was done until an achievable uniformity was obtained. Fourteen combinations of sand and silt were created using clean sand with varying silt contents from 5 to 75% for carrying out cyclic triaxial tests. Clean sand and silt were also used for the testing program.

The scanning electron microscopic view (using FEI-QUANTA 200 scanning electron microscope) of all the materials tested in the laboratory are shown in Fig. 2.

2.4 Index properties of materials used

The index properties including specific gravity, maximum and minimum index void ratios of each of the materials used in this study were determined as per the specifications of IS: 2720 (part-3) - 1980 and IS:2720 (part-14) -1983 and are presented in Tables 1 and 2. In agreement with the findings of Lee and Fitton (1968) and suggestions made by Polito and Martin (2001) the vibratory table tests were used to determine the maximum dry density thus, the minimum index void ratio of various sand-silt mixtures as it gives more repeatable results.

2.5 Limiting silt content

With addition of fines (silt) to sand, it passes from a sand dominated structure to a silt dominated one, through a transition point called as the limiting fines (silt) content (*LFC*). It is the point below which the soil structure is mainly silt contained within a sand matrix whereas beyond this point

Table 1 Index properties of component soils used in this study

Soil type	Clean sand	Quarry dust (Silt)
IS classification symbol	SP	ML
Maximum grain size (mm)	2	0.0747
Mean grain size D_{50} (mm)	0.375	0.037
Minimum grain size (mm)	0.075	0.00063
Uniformity coefficient (C_u)	3.58	7.83
Coefficient of gradation (C_z)	1.163	1.418
Specific gravity (G_s)	2.65	2.67
Minimum index density (kN/m ³)	15.77	10.14
Maximum index density (kN/m ³)	18.66	16.16
Minimum index void ratio (e_{min})	0.42	0.652
Maximum index void ratio (e_{max})	0.68	1.632
Liquid limit (%)	NP	33.75
Plastic limit (%)	ND	32.18
Plasticity index (%)	NP	1.57 (NP)

NP: nonplastic, ND: not determinable

Table 2 Minimum and maximum gross void ratios of various sand-silt mixtures used in this study

Soil type	Minimum gross void ratio (e_{min})	Maximum gross void ratio (e_{max})
Clean sand	0.42	0.68
Sand + 5% Silt	0.32	0.647
Sand + 10% Silt	0.283	0.63
Sand + 15% Silt	0.255	0.62
Sand + 20% Silt	0.23	0.597
Sand + 25% Silt	0.267	0.703
Sand + 30% Silt	0.273	0.723
Sand + 35% Silt	0.296	0.78
Sand + 40% Silt	0.327	0.866
Sand + 45% Silt	0.33	0.97
Sand + 50% Silt	0.37	1
Sand + 60% Silt	0.373	1.1
Sand + 75% Silt	0.5174	1.364
Silt	0.652	1.632

there are enough fines such that the sand grains loose contact with each other. The limiting fines content (LFC) was calculated using the following expression (Hazirbaba 2005)

$$LFC = \frac{W_{fines}}{W_{sand} + W_{fines}} = \frac{G_f e_{ms}}{G_f e_{ms} + G_s (1 + e_{mf})} \quad (1)$$

Where, W_{fines} is the weight of fines and W_{sand} is the weight of sand in a sand-silt mixture. Similarly G_f , G_s , e_{mf} and e_{ms} stand for specific gravity and maximum index gross void ratio of fines and sand

respectively. Using Eq. (1), the limiting silt content for sand-silt mixtures used in this investigation was found to be 21%.

3. Experimental programme

3.1 Specimen preparation

The soil specimens tested were 50 mm in diameter and 100 mm in height. Specimens were prepared as per ASTM D 5311 (Re-approved 1996) guidelines using dry deposition method. For dense specimens, the oven dried soil (quantity by weight) was filled into the rubber membrane lined split mould, which was fixed to the pedestal of the base plate, by means of a funnel having a nozzle of 12 mm diameter with a long spout. To maintain uniform density over the entire range of the specimen height, the soil was prepared in five layers and gently tamped in a symmetrical pattern to the sides of the specimen mould. The number of tamping blows for each layer was pre-assessed for a particular density. The lower layers were prepared at a lesser density than the higher layers to maintain the uniform density throughout. Relative density was varied by 1% per layer. For loose specimens, the spout of funnel with the pre-weighed soil by weight was placed at bottom of the rubber membrane lined split mould and raised slowly along the axis of symmetry of the specimen mould such that the soil was not allowed to have a drop height. The diameter of the specimen was measured to an accuracy of around 0.2 mm at three equal intervals over the entire height of the specimen by means of a vernier periphery tape. Similarly, the height of the specimen was measured to an accuracy of around 1 mm. The height of the soil specimen was kept little more than the desired height of 50 mm so as to get exact height of 50 mm after application of vacuum. A small vacuum of around 20 kPa was applied to the specimen to induce some positive effective stress on it. After the application of vacuum for about one hour, the height of the specimen was again measured to an accuracy of 0.1 mm through the displacement transducer, so that the exact height of 100 mm was possible before saturation and consolidation processes.

3.2 Saturation and consolidation

After specimen preparation was complete and it was formed, CO₂ was passed slowly through the specimen for about 10 to 25 minutes depending on the fines content (more time for specimen with more fines content) followed by de-aired water at a very low gradient (less than five) to get a higher initial saturation. Once a desired volume of water was collected, the specimen was saturated by increasing the back pressure at regular intervals while keeping the effective confining pressure at 30-35 kPa and the Skempton's pore water parameter B ($\Delta u/\Delta\sigma_3$) was periodically monitored until a value of 0.95 (Mullis *et al.* 1978, Ladd 1978) or more was achieved indicating that the specimen was essentially saturated.

Once an acceptable degree of saturation was obtained, the specimens were isotropically consolidated to an effective pressure of 100 kPa. The duration of consolidation was varied from a minimum of 4 minutes for clean sand specimens to a maximum of 90 minutes for pure silt specimens. All the gross void ratios reported in this study are post consolidation gross void ratios and similarly, the relative densities, sand skeleton void ratios, and interfine void ratios were calculated based on these post consolidation gross void ratios.

3.3 Cyclic triaxial testing system

The cyclic resistance of soil specimens was determined by performing cyclic triaxial tests on reconstituted specimens. Testing was carried out using state of the art cyclic triaxial testing apparatus. The equipment consists of a triaxial cell, an LVDT to measure the vertical displacement, a submersible load cell of 5 kN capacity, and three transducers to measure the volume change, chamber pressure, and pore water pressure. The triaxial cell is built with a low friction piston rod seal to which the submersible servo controlled load cell is fitted. The loading system consists of a load frame and hydraulic actuator capable of performing both static and dynamic (strain-controlled as well as stress-controlled) tests, with a frequency range of 0.01 Hz to 10 Hz, employing built-in sine, triangular, and square wave forms. The equipment is computerized and servo-controlled. The cyclic triaxial testing apparatus used is presented in Fig. 3.

3.4 Program of experiments

A detailed program of experiments adopting various approaches as mentioned earlier is presented in a tabular form in Table 3. A total of 241 tests were carried out on reconstituted specimens adopting all these approaches.

3.5 Testing procedure

After the consolidation process was complete, the drainage lines were closed and the LVDT was initialized to zero. The specimens were then, loaded with stress controlled cyclic loading (using a repeating uniform sine wave) and a constant peak deviator stress at the appropriate cyclic stress ratio (*CSR*) with a frequency of 0.1 Hz, until they liquefied. The cyclic stress ratio (*CSR*) is defined as (Eq. 2)



Fig. 3 Cyclic triaxial testing apparatus

Table 3 Programme of experiments

Approach adopted	CGVR (e)/ CRD (%)/ CSSVR(e_s)/ CIVR(e_f)	Soil type	σ'_{3c} (kPa)	Freq (Hz)	Range of cyclic stress ratio (CSR)	Total no of expts
CGVR	$e_c = 0.44$	Sand + 0, 5, 10, 15, 20, 25, 30, 35, 40, 45, 50 & 60% Silt	100	0.1	0.102-0.409	41
CGVR	$e_c = 0.54$	Sand + 0, 5, 10, 15, 20, 25, 30, 35, 40, 45, 50, 60 & 75% Silt	100	0.1	0.056-0.409	47
CRD	$RD_c = 53\%$	Sand + 0, 5, 10, 15, 20, 25, 30, 35, 40, 45, 50, 60, 75% Silt & Silt	100	0.1	0.0165-0.205	48
CSSVR	$e_s = 0.54$	Sand + 0, 5, 10, 12.5 & 15% Silt	100	0.1	0.128-0.358	19
CSSVR	$e_s = 0.607$	Sand + 0, 5, 10, 15, 17.5 & 20% Silt	100	0.1	0.102-0.358	25
CSSVR	$e_s = 0.84$	Sand + 20 & 25% Silt	100	0.1	0.102-0.204	08
CSSVR	$e_s = 1.12$	Sand + 25, 30 & 35% Silt	100	0.1	0.064-0.256	11
CSSVR	$e_s = 1.38$	Sand + 30, 35 & 40% Silt	100	0.1	0.056-0.179	11
CSSVR	$e_s = 1.87$	Sand + 40, 45 & 50% Silt	100	0.1	0.041-0.307	13
CSSVR	$e_s = 2.27$	Sand + 45 & 50% Silt	100	0.1	0.077-0.154	06
CSSVR	$e_s = 2.77$	Sand + 50 & 60% Silt	100	0.1	0.077-0.307	09
CIVR	$e_f = 1.47$	Sand + 20, 30 & 40% Silt	100	0.1	0.154	03

Grand Total No. of Tests = 241

Where, CGVR → constant gross void ratio, CRD → constant relative density, CSSVR → constant sand skeleton void ratio, and CIVR → constant interfine void ratio, and e_c , RD_c , e_s , e_f → represent post consolidation gross void ratio, relative density, sand skeleton void ratio, and interfine void ratio respectively.

$$CSR = \frac{\sigma_{dc}}{\sigma'_{3c}} \quad (2)$$

with the cyclic shear stress (σ_{dc}) being the stress resulting from the peak cyclic load in compression (ΔP_c) and extension (ΔP_e) applied on the specimen of post-consolidation area A_c (Eq. 3)

$$\sigma_{dc} = \frac{\Delta P_c + \Delta P_e}{2A_c} \quad (3)$$

and σ'_{3c} is the effective confining pressure. Initial liquefaction was defined as the state at which the excess pore water pressure in the specimen becomes equal to the initial effective confining pressure. In this study, the cyclic resistance ratio was defined as the cyclic stress ratio (CSR) required to cause initial liquefaction corresponding to 20 cycles of uniform loading.

3.6 Typical test result and discussion

Results from a typical cyclic triaxial test are presented in Fig. 4. The test was carried out on a specimen with 5% silt content at a post consolidation gross void ratio of 0.44. The specimen was loaded at a cyclic stress ratio (CSR) of 0.205 and reached the initial liquefaction at the 41st cycle.

Fig. 4(a) shows the development of axial strains in the specimen with cycles of loading. It can be seen that the initial axial strains developed during cyclic loading in stress mode are small but as the pore water pressure builds up and the soil specimen loses its stiffness, the axial deformation

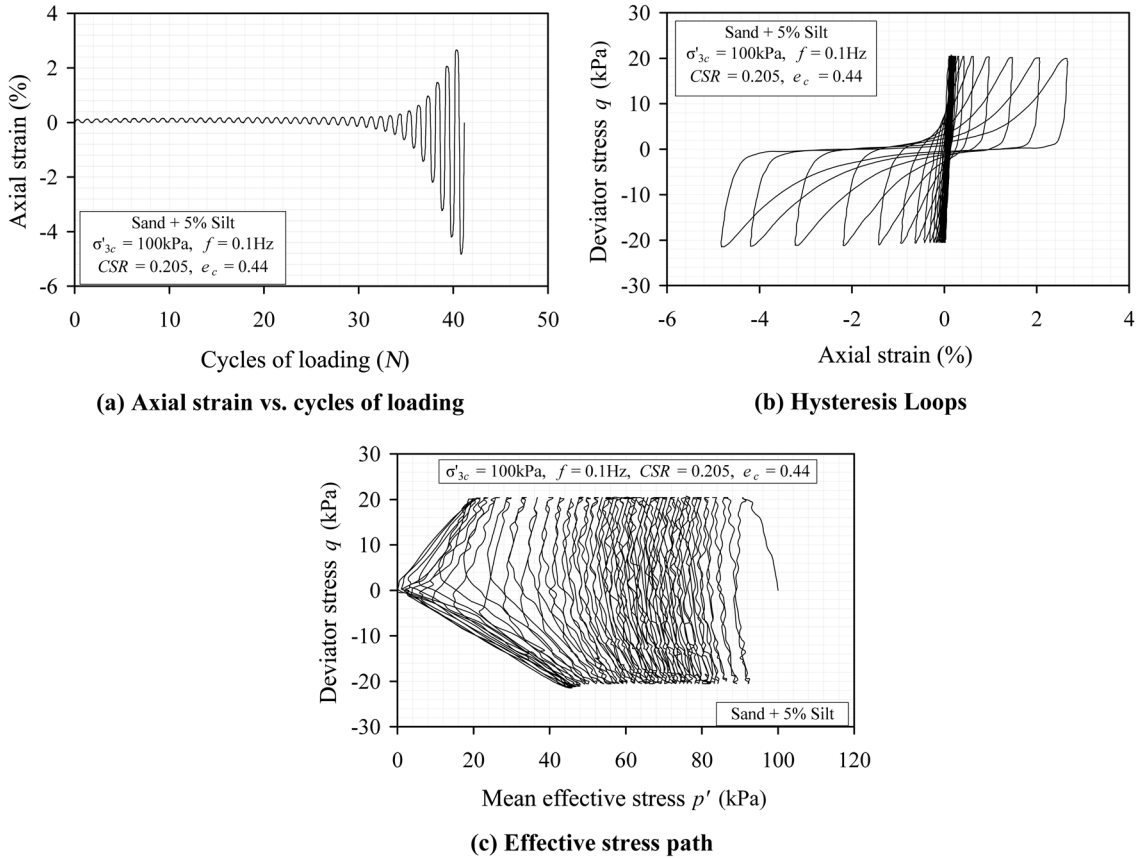


Fig. 4 Typical cyclic test result

increases at a very high rate towards liquefaction. During the entire test programme it was observed that the development of axial deformations increased drastically after around 70% generation of excess pore water pressure in case of liquefaction, but this rate is slowly gained in case of cyclic mobility. It should also be noted that the cumulative permanent axial deformation of the specimen was on the compression side. This finding was almost similar for all the cases. The hysteresis loops obtained from the plots of deviator stress against axial strain are shown in Fig. 4(b) and it is seen that the loops spread in both the directions towards liquefaction while going through the origin. A look at the corresponding stress path (Fig. 4(c)) reveals that it moves gradually towards the origin with effective stress becoming zero at the onset of liquefaction in the 41st cycle. This may be called as the complete cyclic liquefaction of the sample losing all its strength and stiffness. Except for very dense specimens (*Relative Density more than 75%*) where cases of cyclic mobility were observed, all other specimens were seen to loose their strength and stiffness due to complete cyclic liquefaction.

3.7 Determination of cyclic resistance ratio (CRR)

A minimum number of three tests at various cyclic stress ratios (CSR) were conducted on

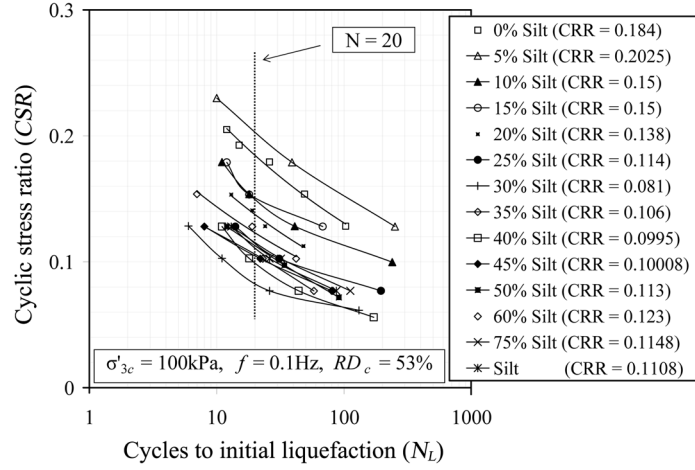


Fig. 5 Cyclic stress ratios vs. cycles to initial liquefaction at $RD_c = 53\%$

isotropically consolidated specimens with a particular silt content and density corresponding to the concerned approach until the specimen was liquefied (i.e. up to initial liquefaction). Then, these cyclic stress ratios were plotted against the corresponding cycles to initial liquefaction (N_L) and from this plot the cyclic resistance ratios (CRR) were evaluated corresponding to 20 cycles of uniform loading (to represent an earthquake of magnitude $M_w = 7.5$, similar to the one which occurred in Bhuj, India earthquake, 2001). A typical CSR vs. N_L plot is presented in Fig. 5 from the test results on specimens prepared to various silt contents at a constant post consolidation average relative density (RD_c) of 53% and the values of CRR obtained from these plots adopting the above mentioned procedure are reported as CRR (in brackets) in this figure. Similar procedure was adopted for all the approaches.

4. Gross void ratio approach

The gross void ratio (e) of a soil specimen is the ratio of the volume of void (V_V) to the volume of the soil solids (V_S) in the specimen. It can be expressed as a function of dry density (γ_d) of the soil specimen and the specific gravity (G_s) of the soil solids. The void ratio (e) of the specimens tested was found to be essentially independent of the silt content, except for the small effect that the amount of silt present has on the specific gravity (G_s) of soil solids. This statement can easily be verified from the expression of dry density (γ_d) of the specimen (Eq. 4)

$$\gamma_d \equiv \frac{G_s \gamma_w}{1+e} \Rightarrow e = \frac{G_s \gamma_w}{\gamma_d} - 1 \Rightarrow e = \frac{G_s \gamma_w}{W_d/V} - 1 \quad (4)$$

As the unit weight of water (γ_w) is generally considered to be unity at normal temperature, the void ratio (e) solely depends on the dry weight (W_d) of the soil used and the volume (V) of the specimen.

Significant researches have been carried out world wide through laboratory tests to evaluate the undrained cyclic response of sandy soils with some amount of silt adopting gross (global) void ratio as the measure of its density. Chang *et al.* (1982), and Amini and Qi (2000) reported that the cyclic

resistance of sand increases with increase in silt content when tested at the same gross void ratio whereas Kuerbis *et al.* (1988) and Finn *et al.* (1994) reported a decrease. Many other investigators (Polito and Martin 2001, Xenaki and Athanasopoulos 2003, Ueng *et al.* 2005, Ravishankar 2006) concluded that the cyclic resistance initially decreases with increase in fines content until a threshold value of silt content (limiting silt content) is reached and then, it increases. Thus, the reported results appear to be conflicting in nature.

In an attempt to clarify the effect of nonplastic fines on the undrained cyclic response of sandy soils, about 88 tests as per the test programme mentioned in Table 3 were performed using stress controlled technique at constant post consolidation average gross void ratios of 0.44 and 0.54. These void ratios were chosen as it was possible to prepare specimens over the entire range of silt contents investigated and to justify the trend at and near the limiting silt content.

4.1 Liquefaction analysis

Fig. 6 plots the cyclic resistance ratio (*CRR*) versus percent silt content at constant gross void ratios (e_c) of 0.44 and 0.54. As may be seen in Fig. 6, the *CRR* decreases rapidly as the silt content increases until a minimum *CRR* is reached at the limiting silt content and with further increase in silt content, it increases up to 50% silt content and beyond this point there is a drastic increase in the *CRR* value. This behaviour is similar for both the gross void ratios chosen. The cyclic resistance ratios at lesser gross void ratio (i.e. $e_c = 0.44$) is found to be more than those with higher gross void ratio (i.e. $e_c = 0.54$) for all the silt contents investigated. The *CRR* corresponding to 60% silt content at gross void ratio (e_c) of 0.44 is found to be more than the *CRR* of clean sand at the same gross void ratio. Similarly, the *CRR* at 75% silt content at gross void ratio (e_c) of 0.54 is almost twice the *CRR* of clean sand at the same gross void ratio. The decrease and subsequent increase in the cyclic resistance ratio can also be attributed to changes in relative densities in the constant gross void ratio approach. The relative density of sand-silt mixtures decreases with increase in silt content until the limiting silt content is reached and thereafter it increases (can be seen in Fig. 7). The sharp rise in *CRR* may be due to sharp rise in relative density (up to about 91% for 60% silt and sand mixture at

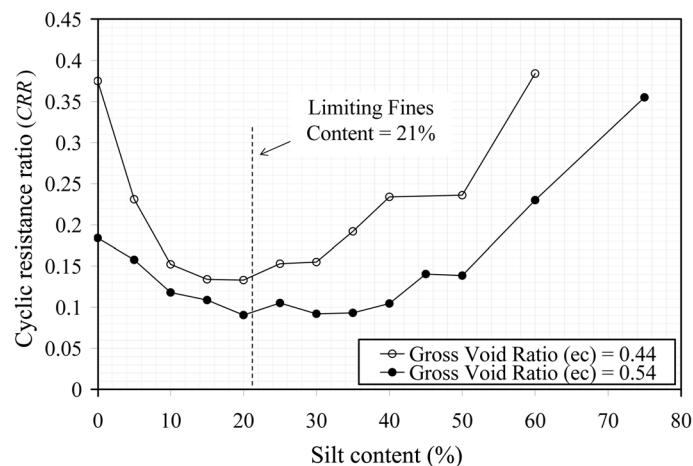


Fig. 6 Cyclic resistance of sand and silt mixture specimens at constant post consolidation average gross void ratios ($e_c = 0.44$ and $e_c = 0.54$) with variation in silt content

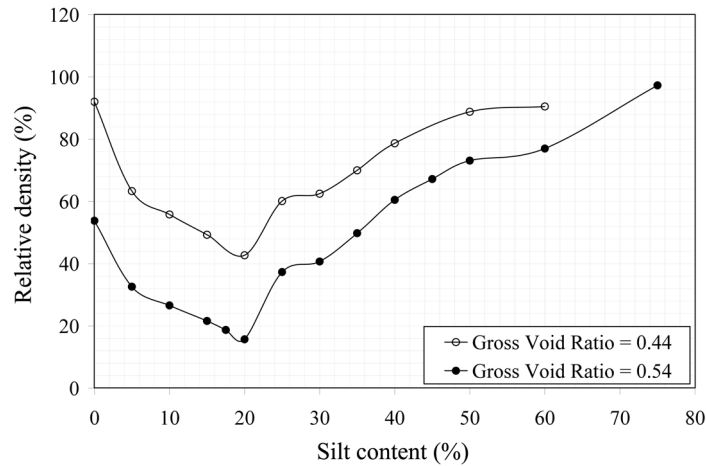


Fig. 7 Variation in relative density with silt content at $e_c = 0.44$ and $e_c = 0.54$

$e_c = 0.44$ and to about 97% for 75% silt and sand mixture at $e_c = 0.54$) beyond the limiting silt content. Also, it should be noted that it was difficult to prepare sand-silt mixture specimens containing 75% silt and pure silt at gross void ratio of 0.44 and for pure silt at gross void ratio of 0.54, as the corresponding relative densities were found to be more than 100%.

At last, the cyclic resistance ratio of each combination of sand and silt was tested at various gross void ratios, which is presented in Fig. 8. It was observed that for a given silt content, when the gross void ratio was varied, the cyclic resistance ratio decreased as the void ratio increased. This behaviour was found to be similar for clean sands also. The general trend for cyclic resistance ratio at all silt contents and at all void ratios derived from various approaches can also be seen in Fig. 8 which clearly shows a decreasing trend of cyclic resistance ratio with increase in void ratio irrespective of the silt content.

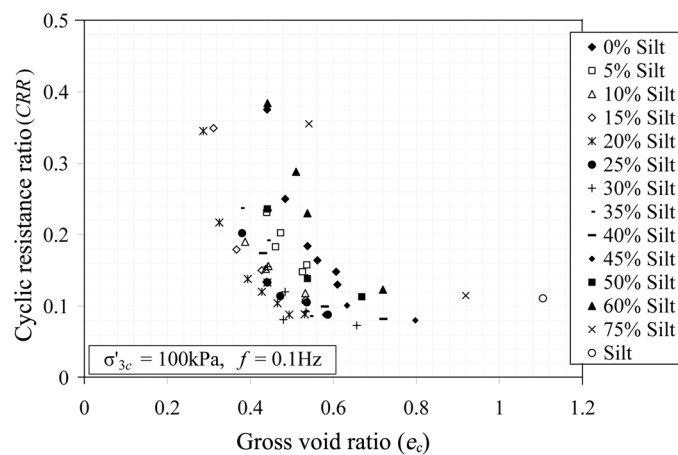


Fig. 8 Variation in cyclic resistance ratio with void ratio at different silt contents

4.2 Pore water pressure analysis

The excess pore pressure developments have been studied with respect to the cycles of loading, and shear strain generated. A typical undrained cyclic pore pressure response plot is shown in Fig. 9, in which a comparison of pore pressure developments in specimens with 0, 10, 20, 35 and 50% silt content are presented for a constant gross void ratio of 0.54 and a constant cyclic stress ratio of 0.128. As may be seen in this figure, the rate of excess pore water pressure generation with respect to cycles of loading increases with increase in silt content until the limiting silt content and then, reverses its trend with further increase in silt content thus, justifying the decreasing to a minimum and then, increasing liquefaction potential of sand-silt mixture specimens at a constant gross void ratio. It can also be observed from this figure that the rate of pore pressure generation in clean sand

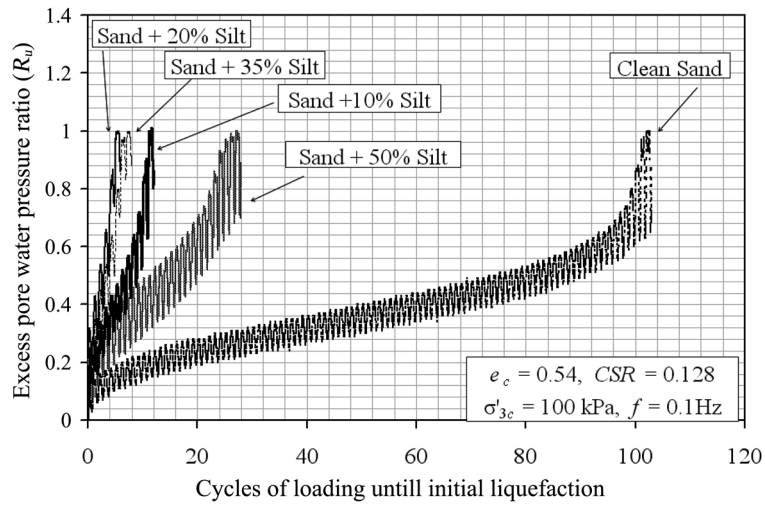


Fig. 9 A typical plot showing excess pore water pressure generation in different silt contents at a constant gross void ratio

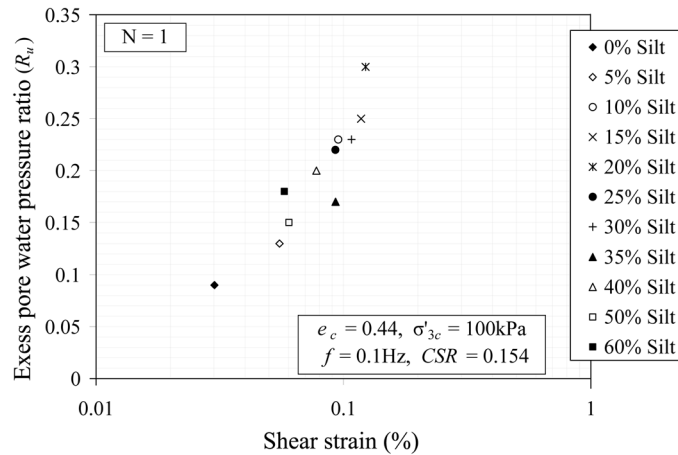


Fig. 10 First cycle pore pressure response against corresponding shear strain at $e_c = 0.44$

is much slower in comparison with sand and silt (10, 20, 35 and 50%) mixture specimens. The excess pore water pressure ratio (R_u) reached the limiting value of 1 in 103 cycles of loading for clean sand whereas for specimens with 10, 20, 35 and 50% of silt content, $R_u = 1$ reached at 11, 6, 7 and 28 cycles of loading respectively under similar conditions.

Next, the pore water pressures generated and the induced shear strains in the first cycle of loading were evaluated to assess the effect of fines content on these developments. These results have been plotted for specimens prepared to constant gross void ratio of 0.44 at cyclic stress ratio of 0.154 in Fig. 10. It is observed that at similar cyclic stress ratio, the first cycle shear strain and corresponding excess pore water pressures are maximum at fines content of 20% and it is minimum for clean sand specimens implying again that the specimens at or near the limiting silt content is the weakest one at a constant gross void ratio. This behaviour was found to be similar at $e_c = 0.54$ (not reported here). It is also observed from Fig. 10 that the excess pore water pressure increases with increase in shear strain irrespective of the fines content. A similar observation was also made (not reported here) at 20th cycle of loading for all fines content at these constant gross void ratios.

5. Relative density approach

Secondly, the undrained cyclic response of sand and silt mixture specimens was evaluated in terms of relative density. The relative density of a specimen is based on the gross void ratio of the specimen and the maximum and minimum index gross void ratios for a particular mixture of sand and silt and is calculated using the following expression.

$$RD = \frac{e_{\max} - e}{e_{\max} - e_{\min}} \quad (5)$$

Where RD is the relative density, e_{\max} and e_{\min} are the maximum and minimum gross void ratios of a particular sand-silt mixture and e is the gross void ratio of the specimen. The relative density is generally expressed as a percentage.

It is well established that the liquefaction potential of a soil specimen increases with increase in the relative density. However, when the soil specimens are tested at a constant relative density with different silt contents, there are controversial conclusions in the literature regarding the nature of variation in cyclic resistance of a specimen. This has compelled many researchers to investigate this aspect more rigorously. Singh (1994) and Chien *et al.* (2002) reported that the cyclic resistance decreases with increase in silt content at a given relative density. However, Polito and Martin (2001) reported that the cyclic resistance remains relatively constant with increase in silt content up to the limiting silt content, and then, there is a drastic fall in cyclic resistance down to a stable level with increase in silt content until pure silt. They also reported that the cyclic resistance below the limiting silt content is at a higher level than that beyond the limiting silt content. Sadek and Saleh (2007) have reported that the cyclic resistance (CRR_{field}) is well understood at a constant relative density if the fines content in a sandy soil is below the limiting silt content. They also reported that the cyclic resistance at a constant relative density increases with increase in fines content and attains a peak at silt content below the limiting silt content, and then, there is a gradual fall in cyclic resistance with increase in silt content and this finding was true for various constant relative densities chosen.

In view of the above conflicting conclusions, an attempt was made to clarify the liquefaction and pore water pressure generation characteristics of sand-silt mixtures at a constant relative density. A post consolidation relative density of 53% was chosen for this purpose as it was found in the other approach i.e. constant gross void ratio approach that the effect of fines is felt considerably for low to medium dense specimens rather than very dense specimens. A total of around 48 tests at a constant post consolidation relative density of 53% as per the programme mentioned in Table 3 were conducted on sand-silt mixture specimens with silt content varying from 0 to 100%.

5.1 Liquefaction analysis

The cyclic resistance ratios (*CRR*) of various specimens tested at a constant post consolidation relative density of 53% were evaluated adopting similar procedure as discussed earlier and are presented in Fig. 11 against the corresponding silt content. As may be seen in Fig. 11, the cyclic resistance ratio at 5% silt content is higher (around 10%) than that of clean sand and this may be

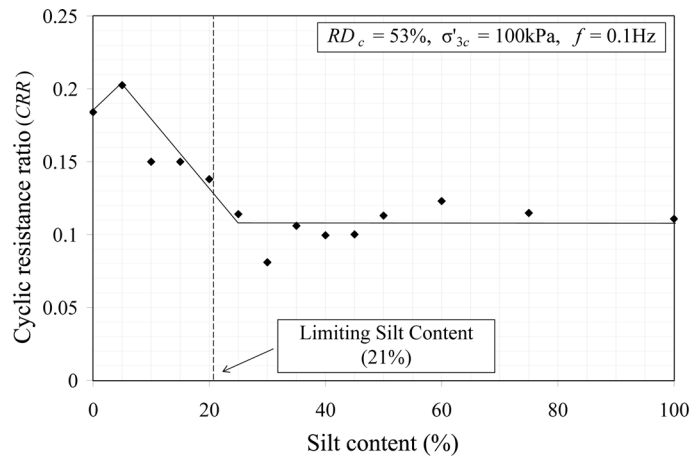


Fig. 11 Variation in cyclic resistance ratio (*CRR*) with silt content at constant relative density ($RD_c = 53\%$)

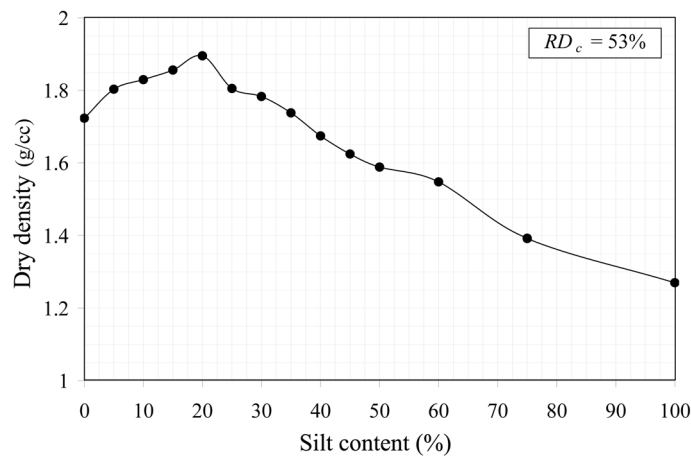


Fig. 12 Variation in dry density with silt content at constant relative density ($RD_c = 53\%$)

due to the fact that the post consolidation dry density (γ_{dc}) of sand and 5% silt mixture at this relative density is more than that of clean sand (Fig. 12), and up to 5% silt content there is no or little influence of fines on the cyclic resistance of sandy soils as reported by many researchers in the past (Seed *et al.* 1985). After attaining the peak at 5% silt content, there is drastic fall in the cyclic resistance ratio until around the limiting silt content. Despite the fact that the dry density of specimens up to the limiting silt content was more than that of clean sand and sand with 5% silt (implying that more weight of soil was contained in the same volume) which may be seen in Fig. 12, but still the cyclic resistance ratio decreased with increase in silt content and the influence of fines during this phase can well be understood in determining the *CRR* at a constant relative density. The drastic fall in cyclic resistance ratio from 5% silt content until the limiting silt content is around 46%. After reaching a minimum value at around the limiting silt content the cyclic resistance ratio remains relatively constant for all combinations of sand and silt, even for pure silt though there is continuous decrease in post consolidation dry density (Fig. 12) after the limiting silt content. The sharp fall in cyclic resistance ratio in constant relative density approach within the region of 5% silt content to around the limiting silt content may be attributed to the unstable sand-silt skeleton and readjustments of sand and silt grains within this region there by weakening the structure of the sample. After readjustments within this region, the sand-silt structures try to become a stable structure after the limiting silt content. As the stability is reached, the cyclic resistance ratio remains relatively constant for all fines content, even for pure silt. It can also be seen that the cyclic resistance ratios of specimens below the limiting silt content is remarkably higher than that of specimens with silt content more than the limiting silt content.

Next, the cyclic resistance ratios were evaluated at all relative densities (derived from various approaches) for all the fines content and are plotted in Fig. 13. It may be seen in this figure (Fig. 13) that the *CRR* increases with increase in relative density irrespective of silt content. The mean variation of these cyclic resistance ratios follows an exponential distribution pattern given by the following equation (Eq. 6)

$$CRR = 0.03 e^{0.0271(RD_c)} \tag{6}$$

Where, *CRR* is the cyclic resistance ratio and RD_c is the post consolidation relative density in this

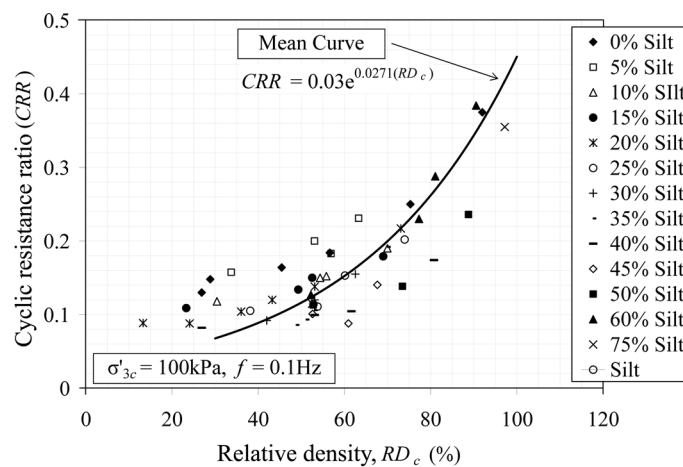


Fig. 13 Variation in cyclic resistance with relative density at different silt contents with distribution patterns

equation. It may also be observed from this figure (Fig. 13) that after around 70% relative density the cyclic resistance ratio of specimens with any silt content increases drastically with a tendency to converge at around 100% relative density despite some minor deviations.

5.2 Pore water pressure analysis

The excess pore water pressures generated during undrained cyclic loading were analyzed as functions of cycles of loading, and shear strain. A typical pore pressure response plot for sand-silt mixture specimens with silt contents of 0, 5, 30, 50 and 100% and at a cyclic stress ratio of 0.128 is presented in Fig. 14. It may be seen from this figure that the sand and 5% silt mixture specimen developed excess pore pressure at slower rate in comparison to other silt contents at a constant relative density and reached $R_u = 1$ at 251 cycles of loading whereas clean sand achieved this in

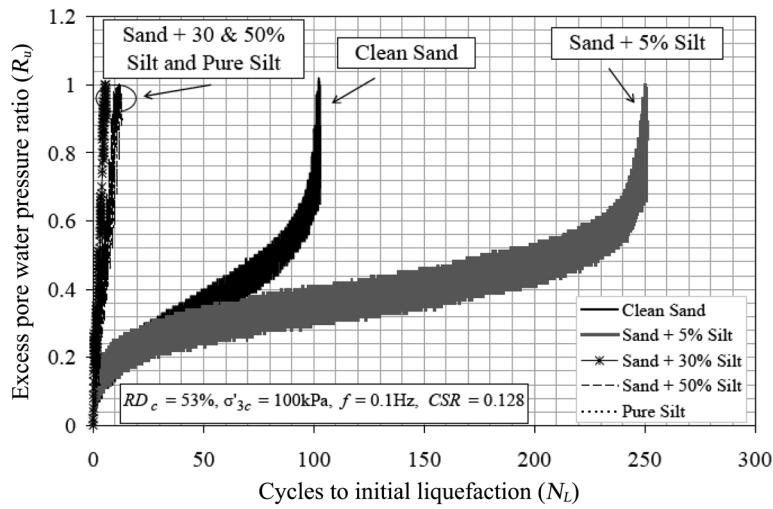


Fig. 14 Typical pore pressure response plot for specimens at different silt contents at $RD_c = 53\%$

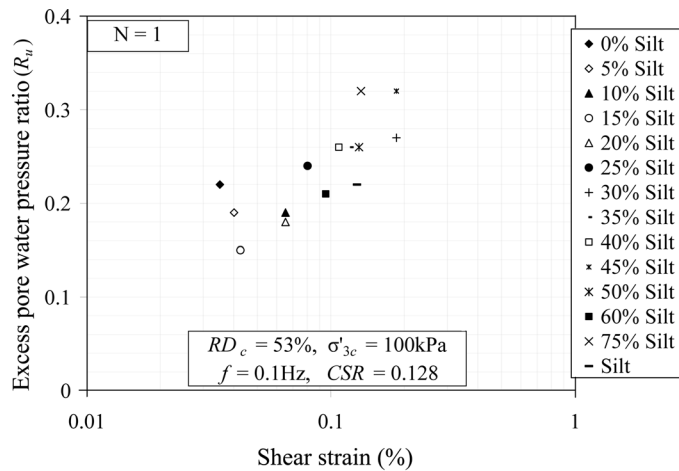


Fig. 15 1st cycle pore pressure response as a function of shear strain ($RD_c = 53\%$)

103 cycles, and specimens with 30 and 50% silt content achieved this in 6 and 12 cycles of loading respectively. Pure silt achieved $R_u = 1$ at 13th cycle. This finding in pore pressure development justifies the cyclic resistance behaviour of sand-silt mixture specimens prepared at a constant relative density.

Next, the peak pore pressures generated during 1st cycle of loading at a cyclic stress ratio of 0.128 in these specimens and the corresponding shear strains were evaluated to assess the effect of fines in generating excess pore water pressures with respect to shear strains. These excess peak pore water pressures are plotted in Fig. 15 against corresponding shear strains. It may be seen in this figure that the specimens with 0 to 20% silt content have generated lesser 1st cycle pore water pressures and shear strains in comparison to specimens at higher silt contents thus, confirming that these specimens have more resistance to liquefaction than the specimens prepared at silt contents greater than the limiting silt content. Also it may be seen in this figure that the pore pressure generation is not proportional to the shear strains below limiting silt content. Specimens with 15% silt content generated less pore water pressure at higher shear strains in comparison to clean sand and specimens with 5% silt content thus, implying that presence of fines resist pore water pressure development when prepared at silt contents below the limiting silt content at a constant relative density. But it is also observed that there is increase in pore water pressure generation with increase in silt content for specimens prepared at silt contents well above the limiting silt content.

6. Sand skeleton void ratio approach

Sand skeleton void ratio is the gross void ratio that would exist in a silty-sand by removing all the silt particles, leaving only the sand and void to form the soil structure. It is expressed in terms of gross void ratio and the fines content (Kenney 1977, Kuerbis *et al.* 1988) as follows (Eq. 7)

$$e_s = \frac{e + FC}{1 - FC} \quad (7)$$

Where e_s is the sand skeleton void ratio, e is the gross void ratio of the specimen and FC is the fines content.

Several researchers in the past have shown that the sand skeleton void ratio controls the undrained cyclic response of a silty sand rather than its gross void ratio, relative density or any other measure of its density. Like the other two approaches already discussed, there is no agreement in the literature regarding the nature of variation in cyclic resistance with increase in silt content at a constant sand skeleton void ratio. Shen *et al.* (1977), Kuerbis *et al.* (1988), Vaid (1994), Polito and Martin (2001), and Xenaki and Athanasopoulos (2003) reported an increasing cyclic resistance with increase in fines content, whereas Finn *et al.* (1994) and Polito and Martin (2001) reported that the cyclic resistance remains constant with increase in fines content at a constant sand skeleton void ratio. It is thus, obvious that different soils respond differently even at similar conditions of testing. In view of these confusions, a total of around 102 tests as per the program mentioned in Table 3 were carried out on isotropically consolidated sand and silt mixture specimens prepared to silt contents both below and beyond the limiting silt content at various possible constant sand skeleton void ratios.

6.1 Liquefaction analysis

Cyclic resistance ratios corresponding to 20 uniform cycles of loading were determined for the specimens prepared to various possible sand skeleton void ratios at silt contents both below and beyond the limiting silt content up to a silt content of 60% adopting the procedure as discussed earlier.

At first the cyclic resistance ratios were analyzed at constant sand skeleton void ratio for specimens prepared below the limiting silt content. For this, post consolidation average sand skeleton void ratio of 0.54 and 0.607 were chosen until a silt content of 15 and 20% respectively. The results are plotted in Fig. 16. It was observed that, below the limiting silt content, the liquefaction potential (in terms of *CRR*) of specimens prepared to constant sand skeleton void ratios of 0.54 and 0.607 remained nearly constant with increase in silt content up to a silt content of 10% and 15% respectively, but the cyclic resistance ratio of sand-silt mixtures with lesser sand skeleton void ratio (i.e. 0.54) was found to be more than that of sand-silt mixtures with higher sand skeleton void ratio (i.e. 0.607). When the cyclic resistance ratios of sand-silt mixtures were evaluated up to a silt content of 15% with the sand skeleton void ratio of 0.54, it was observed that the *CRR* remained unaltered until fines content of about 10% and after that there is a sudden upward jump as is seen in Fig. 16. Similarly, when the *CRR* of sand-silt mixtures was evaluated up to a silt content of 20% with the sand skeleton void ratio of 0.607, it was observed that the cyclic resistance ratio remained unaltered until fines content of about 15% and after that there is a sudden increase in *CRR* as seen in Fig. 16. This sudden gain in cyclic strength of the sand and silt mixtures beyond 10% and 15% silt content at sand skeleton void ratios of 0.54 and 0.607 respectively may be attributed to the rearrangement of soil particles towards a more stable sand-silt structure, thereby offering more resistance to disturbing forces. The other reason may be due to gain in relative density of the soil specimens at constant skeleton void ratio with increase in silt content. For example, at constant sand skeleton void ratio of 0.54, the relative density increases from 57% for clean sand to 70% at 10% silt content, and to about 81% and 84% at 12.5% and 15% silt content respectively (Figs. 16 and 17). Similarly, at constant sand skeleton void ratio of 0.607, the relative density increases from 29% to about 69% and 85% at 15% and 20% silt content respectively.

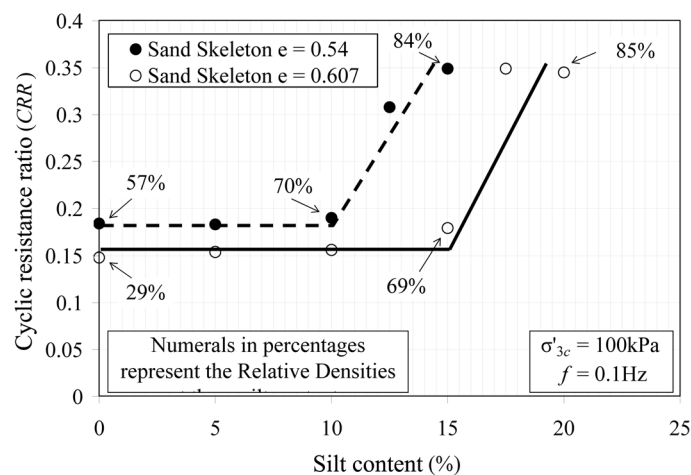


Fig. 16 Variation in cyclic resistance ratio with silt content at constant sand skeleton void ratios of 0.54 and 0.607

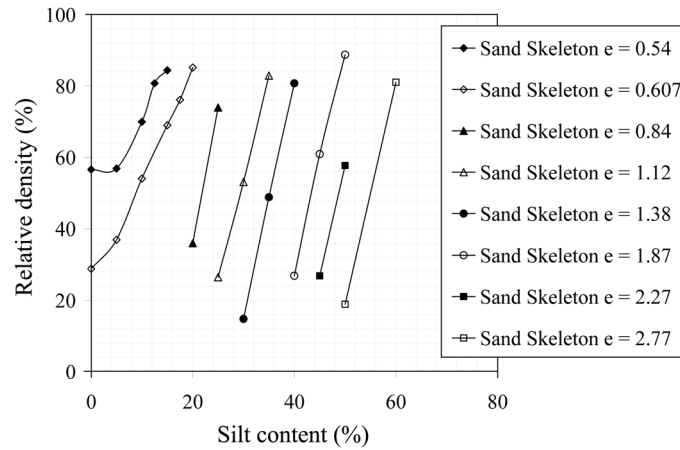


Fig. 17 Variation in relative density with silt content at different sand skeleton void ratios

for clean sand to about 69% at 15% silt content and to about 76% and 85% at 17.5% and 20% silt content respectively which may also be seen in Figs. 16 and 17. This indicates that higher relative densities (more than 70%) make a sand and silt structure more stable and the effect of fines on liquefaction potential at these densities are negligible. It is interesting to note that the relative density of specimen with 12.5% silt content at sand skeleton void ratio of 0.54 is 80.76% and it is more than that of specimens with 17.5% silt content (i.e. 76.14%), but the cyclic resistance ratio of the second specimen is around 13% higher than the first one, thus, indicating that presence of more fines at lower densities resist the process of liquefaction better than that of specimens with less fines content and higher density. It may be noted that the *CRR* of sand-silt mixture with 15% silt content at sand skeleton void ratio of 0.54 and the cyclic resistance ratios of sand-silt mixtures with 17.5% and 20% silt content at sand skeleton void ratio of 0.607 are almost same. Thus, it indicates that the cyclic resistance ratios at higher relative densities are independent of silt content and also the sand skeleton void ratio.

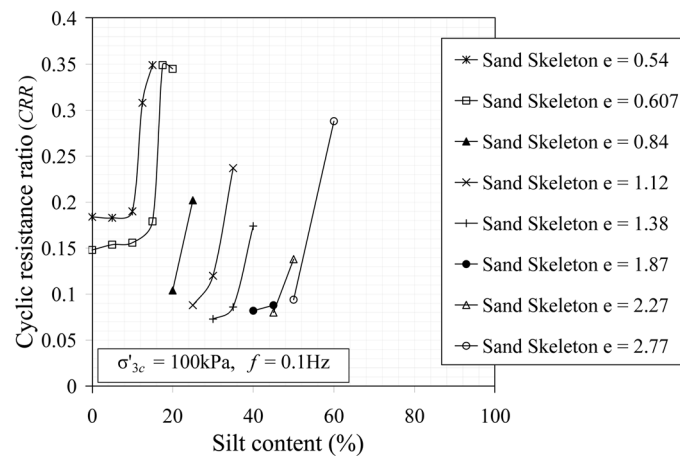


Fig. 18 Variation in cyclic resistance with silt content at different sand skeleton void ratios

Next, the cyclic resistance ratio of specimens with silt contents beyond the limiting silt content up to a silt content of 60% was evaluated at various possible sand skeleton void ratios and is presented in Fig. 18. It was observed that the cyclic resistance ratios increased with increase in silt content at a particular sand skeleton void ratio.

6.2 Pore water pressure analysis

The undrained cyclic pore pressure response of sand and silt mixtures as recorded by the data acquisition system during stress controlled cyclic testing were analyzed at constant and various achievable sand skeleton void ratios to study the rate and magnitude of generation of excess pore water pressure with respect to the cycles of loading, silt content and shear strain.

A typical pore pressure response plot is presented in Fig. 19 for sand and silt mixture specimens prepared to a constant post consolidation average sand skeleton void ratio of 0.607 with 0, 5, 10, and 20% silt content at a cyclic stress ratio of 0.154. Relatively constant and then, drastic increase in cyclic resistance with increase in silt content at a constant sand skeleton void ratio beyond a particular silt content as discussed earlier may be verified from this figure as the specimens up to 10% silt content have generated 100% excess pore pressure water pressure at a relatively same but much less number of cycles in comparison to specimens with 20% silt content. A similar observation was made for all the specimens prepared to all other constant sand skeleton void ratios at silt contents both below and beyond the limiting silt content.

The undrained cyclic pore water pressure response of sand-silt mixture specimens prepared to constant sand skeleton void ratios were also analyzed next, with respect to the silt content. Fig. 20 presents the excess pore water generated during undrained cyclic loading corresponding to 1st, 5th, 10th and 20th cycles of loading in the specimens prepared to constant sand skeleton void ratio of 0.54 at cyclic stress ratios of 0.205. As may be seen in this figure, the pore pressure generated in specimens corresponding to any cycle of loading remains more or less same up to 10% silt content and then, decreases with further increase in silt content. This pore pressure generation behaviour again justifies the relatively constant and then, drastic increase in cyclic resistance after a particular

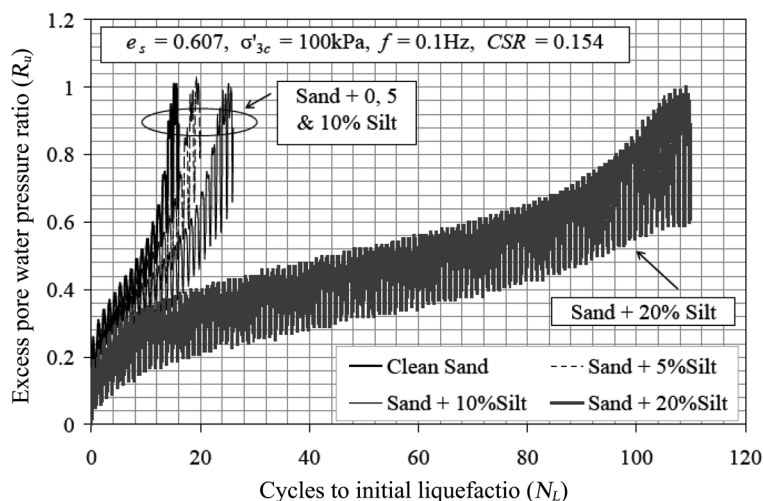


Fig. 19 Typical pore pressure response of specimens with different silt contents at $e_s = 0.607$

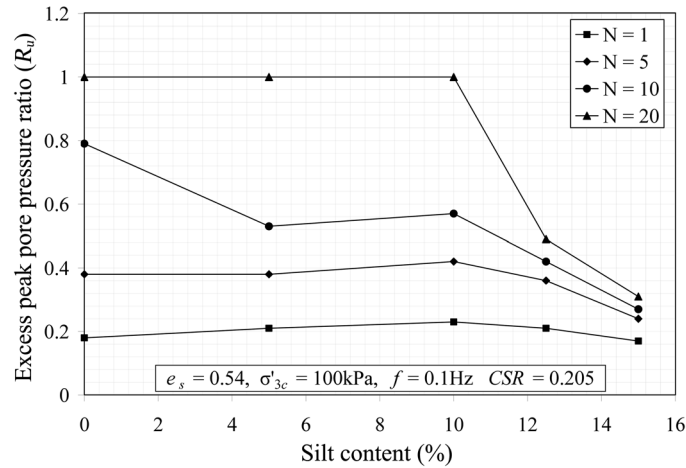


Fig. 20 Pore pressure response as a function of silt content at $e_s = 0.54$

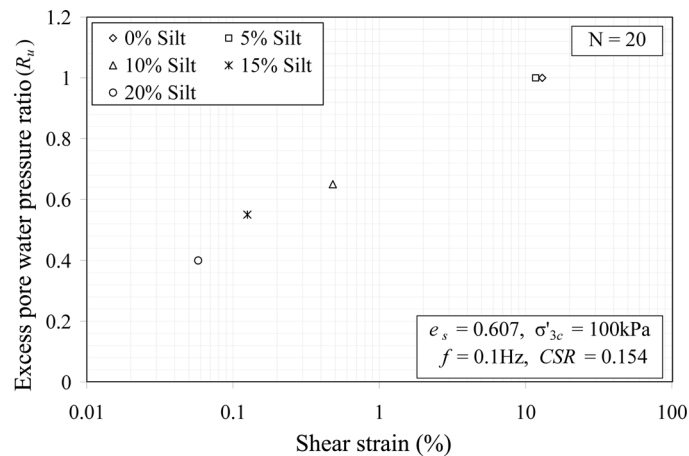


Fig. 21 20th cycle pore pressure response with shear strain at $e_s = 0.607$

silt content in constant sand skeleton void ratio approach which has been discussed earlier. A similar observation was made at all other constant sand skeleton void ratios both below and beyond the limiting silt content.

Next, the excess peak pore water pressure generated during 1st and 20th cycle of loading at various cyclic stress ratios were analyzed with respect to the induced shear strains during these cycles of loading to study the effect of fines content on the generation of excess pore water pressures with respect to shear strains. Fig. 21 presents the pore pressure response with respect to shear strain corresponding to 20th cycle of loading of specimens prepared to constant sand skeleton void ratio of 0.607 at a cyclic stress ratio of 0.154. It may be seen that the densest specimen at this sand skeleton void ratio with silt content of 20% produces the least shear strain and excess pore water pressure in comparison to specimens at other silt contents. Sudden slowing down in shear strain and excess pore water pressure after some silt content can well be seen in this figure thus, justifying the cyclic resistance behaviour in constant sand skeleton void ratio approach. Similar behaviour was observed

at all other constant sand skeleton void ratios both below and beyond the limiting silt content.

7. Interfine void ratio approach

Based on the conceptual framework suggested by Thevanayagam (2001) and substantiated by Xenaki and Athanasopoulos (2003), that the liquefaction behaviour of silty sands beyond the limiting silt content is controlled by the interfine void ratio (e_f) as the silts dominate the soil structure and sands only act as reinforcing material, an attempt was made to study the undrained cyclic response of the sand-silt mixture specimens prepared to silt contents larger than the limiting silt content at a constant post consolidation interfine void ratio of 1.47. The interfine void ratio (e_f) of a sand-silt mixture specimen is defined as the ratio of gross void ratio (e) of the specimen to the corresponding fines content (FC) i.e. $e_f = e/FC$. The specimens with 20, 30, and 40% silt content at a constant post consolidation interfine void ratio of 1.47 were tested with a cyclic stress ratio of 0.154 and a frequency of 0.1 Hz. The initial effective confining pressure applied was 100 kPa. The detailed analysis is presented below.

7.1 Liquefaction analysis

The test result on the above mentioned specimens at a cyclic stress ratio of 0.154 is plotted in Fig. 22. It is observed that the number of cycles required to cause initial liquefaction decreases with increase in silt content implying that the liquefaction resistance decreases with increase in silt content at a constant interfine void ratio. This behaviour is justified as the corresponding relative density decreases with increase in silt content at a constant interfine void ratio which is presented in Table 4. Xenaki and Athanasopoulos (2003) reported similar cyclic resistance behaviour of specimens with silt contents larger than the limiting silt content and prepared to constant interfine void ratio.

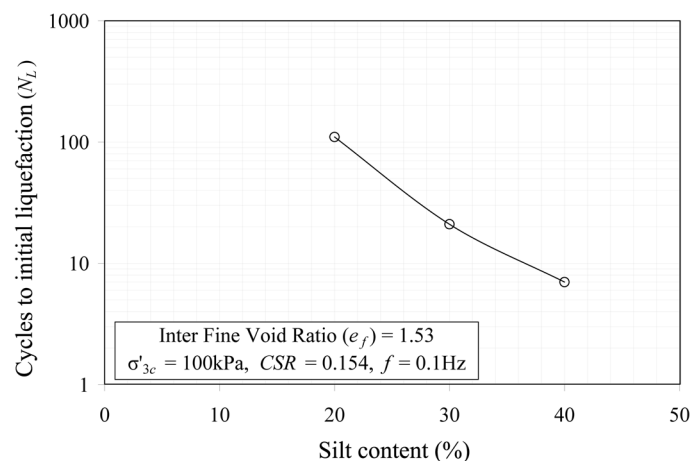
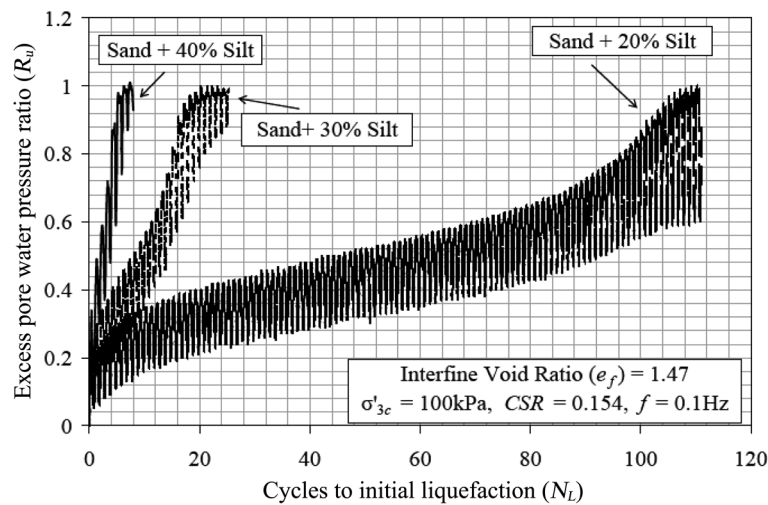


Fig. 22 Cycles to initial liquefaction vs. silt content at $e_f = 1.47$

Table 4 Variation in relative density at $e_f = 1.47$

Silt content (%)	RD_c (%) at $e_f = 1.47$
20	82.42
30	60.46
40	51.96

Fig. 23 Pore pressure ratio vs. cycles of loading at $e_f = 1.47$

7.2 Pore water pressure analysis

The above mentioned liquefaction behaviour was justified from the pore water pressure generation characteristics which is presented in Fig. 23. As seen in this figure, the rate of generation of excess pore water pressure in specimens prepared to constant interfine void ratio and at a constant cyclic stress ratio increases very fast with respect to the cycles of loading as the silt content increases implying that the specimens at higher silt contents at a constant interfine void ratio are weaker in withstanding cyclic loads.

8. Conclusions

Sand structure is completely changed with the addition of fines, and as a result the dynamic responses of sandy soils are also changed. But the manner in which the presence of fines in sand influences these responses has been a matter of discussion until now, with confusing conclusions in the literature regarding the liquefaction behaviour of silty sands. 241 undrained cyclic triaxial test results was utilized in this study in an attempt to clarify some of the anomalies in the literature regarding the liquefaction and pore water pressure generation characteristics of silty sands. The tests were performed at various measures of sample density through several approaches namely gross void ratio approach, relative density approach, sand skeleton void ratio approach, and interfine void

ratio approach. The major conclusions drawn from the present study are summarized below:

1. Specimens prepared at silt contents close to the limiting silt content were found to be weaker in withstanding the cyclically induced loads than their counterparts at silt contents far away from the limiting silt content when the results were interpreted in terms of constant gross void ratio. This behaviour was found to be due to a lesser relative density of these specimens. The specimens at very high silt contents were seen to offer much more cyclic resistance than even clean sands due to their very high relative density. Relative density rather than the silt content is found to be a major player in this approach. The cyclic resistance ratio of specimens was found to have a general decreasing trend with increase in gross void ratio irrespective of the silt content.

2. With an initial increase until 5% silt content due to an increase in dry density of the specimens the cyclic resistance ratio falls drastically until around the limiting silt content and thereafter it remains stable with further increase in silt content when the specimens were tested at a constant relative density. However, the cyclic resistance of specimens at silt contents beyond the limiting silt content was seen to be markedly lower than their counterparts at silt contents below the limiting silt content. The cyclic resistance ratio was seen to increase with increase in relative density irrespective of the silt content but after around 70% relative density it was found to increase drastically with a tendency to converge at around 100% relative density despite some minor deviations. However, at lower relative densities (i.e. $RD_c \leq 70\%$) cyclic resistance ratios were found to be widely scattered over a wider band.

3. Cyclic resistance behaviour of sand and silt mixture specimens prepared to constant sand skeleton void ratio was found to be unique. It remained unaltered with increase in silt content until some silt content corresponding to a relative density of 70% and thereafter, a sudden increase was observed indicating that the cyclic resistance of very dense specimens is independent of either silt content or any approach. Similar observation was made at silt contents both below and beyond the limiting silt content. The cyclic resistance ratio was found to have a general decreasing mode with increase in sand skeleton void ratio irrespective of silt content.

4. It was observed that the cyclic resistance, of specimens with silt contents more than the limiting silt content, decreased with increase in silt content when tested at a constant interfine void ratio. This behaviour was due to a corresponding decrease in relative density.

5. All the cyclic resistance behaviour through any approach were justified by the excess pore water pressure generations with respect to either cycles of loading, silt content or shear strains.

9. Implications of the present finding

From the entire test results, it is finally, concluded that the relative density rather than any approach or silt content (below, at, and beyond the limiting silt content) of a specimen controls the cyclic response of sand-silt mixtures. With addition of fines to a sand, the relative density either increases or decreases at a particular measure of density through any approach (except constant RD approach) and this controls the cyclic strength parameters as well as pore water responses. It is also observed that, the effect of fines is felt prominently in reducing the cyclic strengths of specimens at relative densities lesser than 70% corresponding to any approach. Very dense specimens with any silt content (even at limiting fines content) through any approach seem to produce reasonably higher strengths even more than that of clean sands. Finally, it is suggested that silty sand deposits with any silt content should be densified to the maximum possible limit to impart better strength and

stability to structures founded on them.

Acknowledgements

This investigation was carried out with the sponsorship from Ministry of Earth Sciences, formerly Department of Science and Technology (Seismology Division), Ministry of Science and Technology, Government of India. The authors express their sincere appreciation to the ministry.

References

- American Society for Tests and Materials (ASTM), *Standard test method for load controlled cyclic triaxial strength of soil*, ASTM D 5311-92 (Re-approved 1996), ASTM, West Conshohoken, Pa.
- Amini, F. and Qi, G.Z. (2000), "Liquefaction testing of stratified silty sands", *J. Geotech. Geoenviron. - ASCE*, **126**(3), 208-217.
- Chang, N.Y., Yeh, S.T. and Kaufman, L.P. (1982), "Liquefaction potential of clean and silty sands", *Proceedings of the 3rd International Conference on Earthquake Microzonation*, **2**, 1017-1032.
- Chien, L.K. and Oh, Y.N. (2002), "Influence of fines content and initial shear stress on dynamic properties of hydraulic reclaimed soil", *Can. Geotech. J.*, **39**, 242-253.
- Dash, H.K. (2008), "Undrained cyclic and monotonic response of sand-silt mixtures", PhD thesis submitted to Indian Institute of Science, Bangalore (India) in the Faculty of Engrg.
- Dash, H.K., Sitharam, T.G. and Baudet, B. (2010), "Influence of non-plastic fines on the response of a silty sand to cyclic loading", *Soils and Foundations, JPN Geotech. Soc.*, **50**(5), 695-704. doi:10.3208/sandf.50.695, JOI JST.JSTAGE/sandf/50.695.
- Finn, W.D.L., Ledbetter, R.H. and Wu, G. (1994), "Liquefaction in silty soils: design and analysis", *Ground failures under seismic conditions*, GSP 44, ASCE, New York, 51-76.
- Hazirbaba, K. (2005), "Pore pressure generation characteristics of sands and silty sands: a strain approach", Dissertation presented for PhD program to the faculty of Graduate School at the University of Texas at Austin, 2005.

IS Codes (Bureau of Indian Standards)

IS: 1498-1970	Classification and identification of soils. 1992
IS: 2720	(Part 3) Section 1 - 1980. Specific gravity-fine grained soils. (1992) Section 2 - 1980. Specific gravity-fine, medium and coarse grained soils. (1992)
	(Part 4) - 1985. Grain size analysis. (1995)
	(Part 5) - 1985. Determination of liquid and plastic limit. (1995)
	(Part 14) - 1983. Determination of density index (relative density) of cohesionless soils.

- Kenny, T.C. (1977), "Residual strength of mineral mixtures", *Proceedings of the 9th International conference on Soil Mech. and Found. Eng.*, Tokyo, **1**, 155-160.
- Kuerbis, R., Nigussey, D. and Vaid, Y.P. (1988), "Effect of gradation and fines content on the undrained response of sand", *Proceedings on Hydraulic Fill Structures*, GSP No. 21, ASCE, 330-345.
- Ladd, R.S. (1978), "Preparing test specimens using undercompaction", *Geotech. Test. J.*, **1**(1), 16-23.
- Lade, V.P. and Yamamuro, J.A. (1997), "Effects of nonplastic fines on static liquefaction of sands", *Can. Geotech. J.*, **34**, 918-928.
- Lee, K.L. and Fitton, J.A. (1968), *Factors affecting the cyclic loading strength of soil*, Vibration effects of earthquakes on soils and foundations, STP 450, ASTM, West Conshohocken, Pa., 71-95.
- Mullis, J.P., Townsend, F.C. and Horz, R.C. (1978), "Triaxial testing techniques and sand liquefaction", *Dynamic Geotech. Testing*, Edited by Silver and Tiedmann. ASTM Spl. **654**, 265-279.

- Naeini, S.A. and Baziar, M.H. (2004), "Effect of fines content on steady state strength of mixed and layered specimens of a sand", *Soil Dyn. Earthq. Eng.*, **24**, 181-187.
- Polito, C.P. and Martin, J.R. (2001), "Effects of nonplastic fines on the liquefaction resistance of sands", *J. Geotech. Geoenviron.*, **127**(5), 408-415.
- Ravishankar, B.V. (2006), "Cyclic and monotonic undrained behavior of sandy soils", PhD thesis submitted to Indian Institute of Science, Bangalore in the Faculty of Engineering.
- Sadek, S. and Saleh, M. (2007), "The effect of carbonaceous fines on the cyclic resistance of poorly graded sands", *J. Geotech. Geolog. Eng.*, **25**(2), 257-264.
- Seed, H.B., Tokimatsu, K.L.F., and Chung, R. (1985), "Influence of SPT procedures in soil liquefaction resistance evaluations", *J. Geotech. Eng. - ASCE*, **111**(12), 861-878.
- Shen, C.K., Vrymoed, J.L. and Uyeno, C.K. (1977), "The effects of fines on liquefaction of sands", *Proceedings of the 9th International Conference on Soil Mech. and Found. Eng.*, Tokyo, Japan, **2**, 381-385.
- Singh, S. (1994), "Liquefaction characteristics of silts", *Ground Failure Under Seismic Conditions*, GSP **44**, ASCE, 105-116.
- Thevanayagam, S. (1998), "Effect of fines and confining stress on undrained shear strength of silty sands", *J. Geotech. Geoenviron.*, **124**(6), 479-491.
- Thevanayagam, S. (2000), "Liquefaction potential and undrained fragility of silty soils", *Proceedings of 12th World Conference on Earthquake Eng.*, Auckland, New Zealand, p. 8.
- Ueng, T.S., Sun, C.W. and Chen, C.W. (2004), "Definition of fines and liquefaction resistance of Maoluo river soil", *Soil Dyn. Earthq. Eng.*, **24**, 745-750.
- Vaid, Y.P. (1994), "Liquefaction of silty soils", *Ground Failure Under Seismic Conditions*, GSP **44**, ASCE, New York, 1-16.
- Xenaki, V.C. and Athanasopoulos, G.A. (2003), "Liquefaction resistance of sand-silt mixtures: an experimental investigation of the effect of fines", *Soil Dyn. Earthq. Eng.*, **23**, 183-194.

PL